Published October 20, 2014

Dyskerin, tRNA genes, and condensin tether pericentric chromatin to the spindle axis in mitosis

Chloe E. Snider,[1] Andrew D. Stephens,[1] Jacob G. Kirkland,[2] Omar Hamdani,[2] Rohinton T. Kamakaka,[2] and Kerry Bloom[1]

[1]Department of Biology, University of North Carolina at Chapel Hill, Chapel Hill, NC 27599
[2]Molecular, Cell and Developmental Biology, University of California, Santa Cruz, Santa Cruz, CA 95064

Condensin is enriched in the pericentromere of budding yeast chromosomes where it is constrained to the spindle axis in metaphase. Pericentric condensin contributes to chromatin compaction, resistance to microtubule-based spindle forces, and spindle length and variance regulation. Condensin is clustered along the spindle axis in a heterogeneous fashion. We demonstrate that pericentric enrichment of condensin is mediated by interactions with transfer ribonucleic acid (tRNA) genes and their regulatory factors. This recruitment is important for generating axial tension on the pericentromere and coordinating movement between pericentromeres from different chromosomes. The interaction between condensin and tRNA genes in the pericentromere reveals a feature of yeast centromeres that has profound implications for the function and evolution of mitotic segregation mechanisms.

Introduction

Condensin is a DNA compaction machine that functions in chromosome architecture, nucleolar organization, and chromosome segregation (Hirano, 2006). Condensin can introduce supercoils and decatenate topologically linked circles. The most prominent sites of condensin localization in the nucleus are the nucleolus, pericentric chromatin, and central axis of condensed metaphase chromosomes. Condensin is also essential for mechanisms of force balance between the pericentromere heterochromatin and spindle microtubules in metaphase (Stephens et al., 2011, 2013a). Condensin interacts with several key transcription factors, including RNA polymerase III transcription factors (TFIIIC and TFIIIB; Haeusler et al., 2008). This interaction is responsible for the enrichment of tRNA genes to the nucleolar periphery observed in budding yeast. Recently, it has been shown that the monopolin complex recruits condensin to the pericentromere (Brito et al., 2010; Burrack et al., 2013). The monopolin complex is sequestered in the nucleolus until the onset of anaphase, in which it migrates to the kinetochore (Brito et al., 2010; Burrack et al., 2013). In meiosis, monopolin is thought to cross-link sister kinetochores to ensure that sister chromatids segregate to the same pole. None of the known mechanisms attributed to condensin indicate how it functions in force balance in metaphase.

Budding yeast lacks canonical pericentric heterochromatin observed in most organisms. Centromeres in *Saccharomyces cerevisiae* are specified in a site-specific manner (point centromere) but share several features of the surrounding pericentric chromatin characteristic of that found in multicellular organisms. Condensin and cohesin are enriched 3× in the 30–50-kb region surrounding the point centromere (Blat and Kleckner, 1999; Megee et al., 1999; D'Ambrosio et al., 2008). tRNA genes, found in the pericentric regions of many organisms (Kuhn et al., 1991; Iwasaki and Noma, 2012), are enriched 1.8× in the pericentromere of budding yeast (32/307 tRNA genes in the 50 kb surrounding the CEN [centromere] sequence in the 16 chromosomes). tRNAs are modified by several factors, including dyskerin. Dyskerin binds to and stabilizes small noncoding RNAs, which together with other components (H/ACA small nucleolar RNP [snoRNP]) catalyzes the conversion of uridine to pseudouridine in nascent ribosomal RNA and tRNA (Hoang and Ferré-D'Amaré, 2001). Dyskerin is a component of telomerase and is required for telomere maintenance in humans (Gu et al., 2009; Gardano et al., 2012). Dyskerin has been localized to the

Correspondence to Kerry Bloom: Kerry_Bloom@unc.edu

Abbreviations used in this paper: IP, immunoprecipitation; LacO, lactose operon; LTR, long terminal repeat; rDNA, ribosomal DNA; snoRNP, small nucleolar RNP; TetO, tetracycline operon; WT, wild type.

Supplemental Material can be found at:
http://jcb.rupress.org/content/suppl/2014/10/15/jcb.201405028.DC1.html

The Rockefeller University Press $30.00
J. Cell Biol. Vol. 207 No. 2 189–199
www.jcb.org/cgi/doi/10.1083/jcb.201405028

Published October 20, 2014

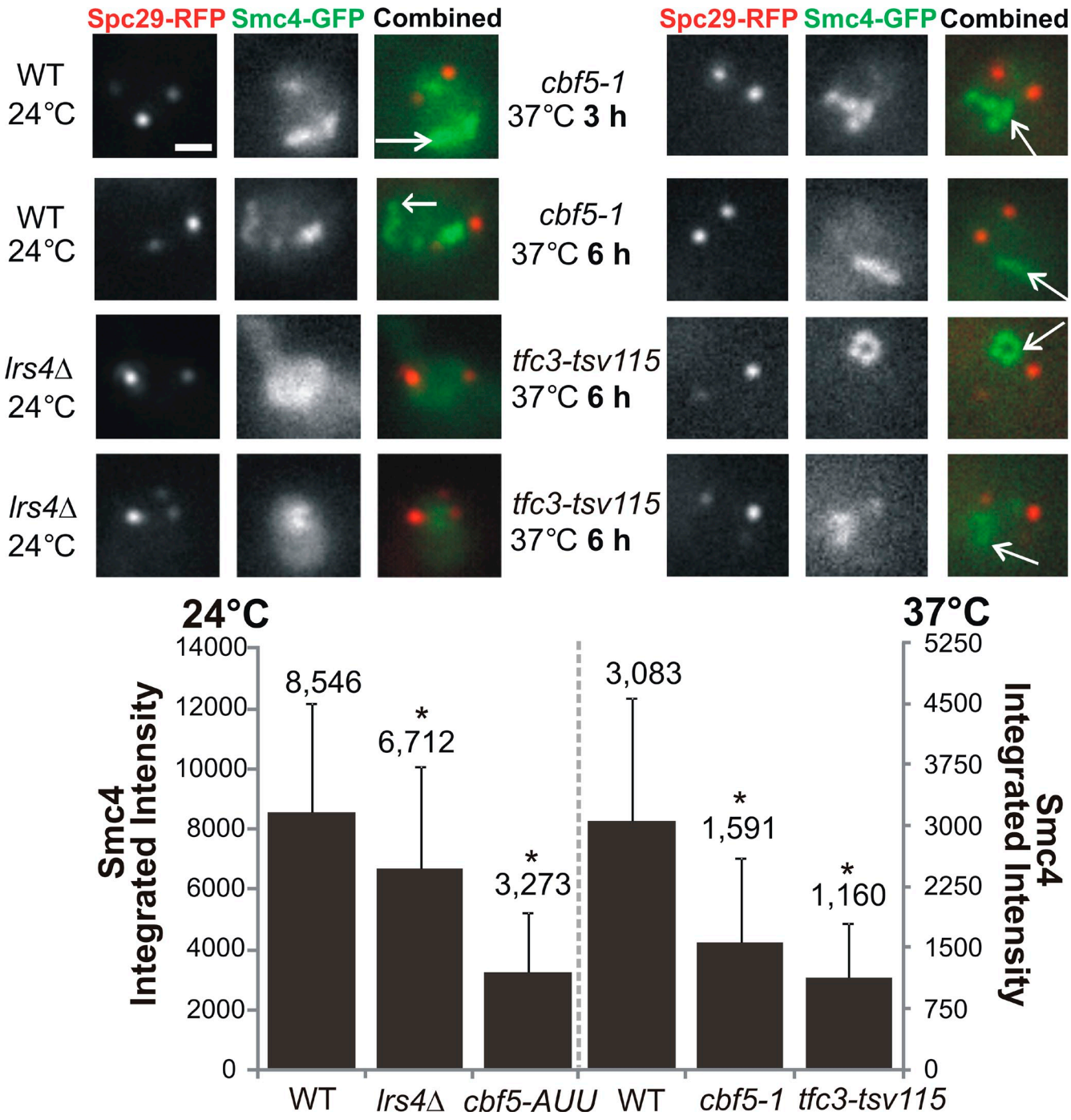

Figure 1. **Pericentric condensin enrichment in WT, monopolin, *cbf5*, and *tfc3* mutant cells.** Condensin (Smc4-GFP) and spindle pole bodies (Spc29-RFP) were imaged at 24°C or after shift to 37°C for 6 h. Representative cells are shown in the top images. Arrows indicate the rDNA locus. (bottom) Integrated intensity of Smc4-GFP between spindle pole bodies (Spc29-RFP) in metaphase cells at 24°C in WT (n = 36), *lrs4Δ* (n = 33), and *cbf5-AUU* (n = 39) cells. WT (n = 32), *cbf5-1* (n = 21), and *tfc3-tsv115* (n = 55) after 6 h at 37°C are shown. *, $P < 0.05$, t test; error bars represent standard deviation. Bar, 1 µm.

mitotic spindle in human cells and shown to be required for faithful chromosome segregation (Alawi and Lin, 2013).

The yeast homologue of dyskerin, CBF5 was discovered in a biochemical assay for centromere binding factors (Jiang et al., 1993). Overexpression of *CBF5* can partially suppress a temperature-sensitive mutation in *cbf2/ndc l0* encoding the ll0-kD subunit of the Cbf3 kinetochore complex (Jiang et al., 1993). Furthermore, Cbf5 has a C-terminal repeat 10× (KKE/DX) motif, conserved in several microtubule binding proteins (MAP1A and MAP1B). In this report, we demonstrate that Cbf5, together with tRNA genes within the pericentromere, is responsible for condensin accumulation along the spindle axis. This provides a mechanism for the physical segregation of condensin from cohesin in single cells and elucidates the role of condensin in mitotic force balance.

Published October 20, 2014

Results and discussion

Enrichment of condensin along the metaphase spindle axis requires both monopolin and dyskerin

In metaphase, condensin (Smc4-GFP) is localized to both ribosomal DNA (rDNA; nucleolus) and the pericentric chromatin surrounding the spindle microtubules in mitosis. The rDNA is organized as a chromatin loop, often juxtaposed to the nuclear envelope (Fig. 1, arrows). Pericentric condensin appears as a focus or line of fluorescence between the spindle poles. In the absence of the major subunit of monopolin (*lrs4Δ*), there is a 20% reduction in the level of Smc4 associated with the pericentric chromatin. The remaining condensin appears heterogeneous along the spindle axis or radially dispersed (Fig. 1, *lrs4Δ* left bottom images).

Because tRNA genes are enriched in the pericentromere in budding yeast, we asked whether regulators of tRNA expression or modification enzymes, such as Cbf5, might recruit condensin to the metaphase spindle. Depletion of *CBF5* results in a 50% reduction of Smc4 associated with the pericentric chromatin (Fig. 1, *cbf5-1* top right images). In contrast to *lrs4Δ* mutants, condensin is not depleted from the rDNA in *cbf5-1* (Fig. S1 C). To separate the essential tRNA modification function from Cbf5's role in condensin localization, we used a nonessential mutation in the first AUG codon to AUU previously identified to alleviate repression by tRNA genes (*art1-1*; Kendall et al., 2000). This mutant affects Cbf5 expression levels and disrupts the nucleolar localization of tRNA genes (Kendall et al., 2000). The concentration of condensin along the spindle axis in metaphase was reduced 60% in the *cbf5-AUU* mutant (Fig. 1, bottom). The localization of condensin in the nucleolus was unperturbed (Fig. S1, C and D). Because Cbf5 is part of the H/ACA box snoRNP complex (Nop10, Nhp2, and Gar1), we asked whether their depletion would affect spindle condensin. We placed Nop10 and Nhp2 under the control of the GALL promoter (Mumberg et al., 1994) and quantitated Smc4-GFP intensity along the spindle axis (Fig. S1). Smc4-GFP is reduced to ∼50% the levels after repression of either Nop10 or Nhp2 (Fig. S1 A). Thus, Cbf5 and the H/ACA box snoRNP complex are responsible for the majority (60%) of condensin recruitment to the mitotic spindle in metaphase.

To test whether RNA polymerase III transcription factors are involved in condensin recruitment, we used a mutation in a polymerase III transcription initiation factor (TFIIIC), *TFC3*. There was a 60% reduction in Smc4-GFP associated with the spindle in a *tfc3-tsv115* mutant (Fig. 1, bottom right bar). As with *cbf5-AUU*, the localization of condensin in the nucleolus was unperturbed in *tfc3-tsv115* (Fig. S1 C). Loss of TFIIIC leads to the reduction of condensin binding to these sites and therefore depletion in the pericentromere.

The reduction of condensin within the pericentromere in monopolin and dyskerin mutants results in a slight increase in spindle length (∼1.8 µm) relative to wild type (WT; ∼1.5 µm) but not as dramatic as the complete loss of condensin in *brn1-9* mutants (2.3 µm; Table 1). To differentiate the role of monopolin and *CBF5* in condensin localization within the pericentromere, line scans were drawn between the spindle poles in cells expressing Smc4-GFP in WT, *lrs4Δ*, or *cbf5-AUU* mutants (Fig. 2). The peak intensity of each line scan was binned into two zones, representing pole proximal (Fig. 2 B, green) and the central spindle axis (Fig. 2 B, blue). In the absence of monopolin, residual condensin localizes to the midspindle 83% of the time compared with 78% in WT (Fig. 2 B). In the *cbf5-AUU* mutant, condensin midspindle localization decreased, and pole-proximal localization increased significantly (Fig. 2 B). Representative images indicate the central spindle axis localization in monopolin mutants and a single focus that is proximal to the pole in *cbf5-AUU* (Fig. 2 A). Monopolin contributes disproportionally to the fraction of condensin proximal to the pole (only 50% central zone localization in *cbf5-AUU* mutant), whereas Cbf5 is responsible for condensin's distribution along the spindle axis in metaphase (83% central axis in *lrs4Δ* mutant).

Table 1. **Spindle length increases in monopolin and cbf5 mutants, and spindle height increases in the cbf5 mutant**

Strain	Mean	Standard deviation	*n*
Spindle length	*µm*		
WT	1.4	0.21	47
lrs4Δ	1.8[a]	0.52	81
cbf5-1 3 h TS	1.9[a]	0.41	121
cbf5-1 6 h TS	2.4[a]	0.55	84
brn1-9[b]	2.3[a]	0.40	80
Spindle height	*nm*		
WT	517	39	103
cbf5-1 6 h TS	583[a]	77	63

TS, temperature sensitive.
[a]Statistically different.
[b]Stephens et al., 2011.

In live cells, Cbf5 is concentrated in the nucleolus (Fig. S2 A). To test whether Cbf5 is involved in condensin recruitment to the pericentromere, we performed chromatin immunoprecipitation (IP) in cells containing Cbf5-GFP (Fig. 2 C). There is a 2.4-fold enrichment of Cbf5 at the pericentromere (*CEN3*) versus an arm locus (*HTB1*; Fig. 2 C, left). Likewise, there is a significant loss of condensin from the pericentromere in the *cbf5-1* mutation (Fig. 2 C, right). Thus, Cbf5 physically associates with pericentric chromatin and is responsible for aggregation of condensin to the spindle axis.

Proper distribution of condensin is required for kinetochore clustering in metaphase

Kinetochores from each of the 16 chromosomes are clustered into sister foci in a condensin-dependent fashion (Stephens et al., 2011, 2013a). Reducing the concentration of condensin in monopolin and dyskerin mutants might have a similar effect on kinetochore clustering. In ∼47% of mutant cells, the outer kinetochore protein Nuf2-GFP was no longer clustered into a close to diffraction focus (Fig. 3, A and C). Likewise, in greater than half of cells, the inner kinetochore protein Cse4-GFP was no longer clustered along the spindle axis (Fig. 3, B and D). The kinetochores were either declustered (as defined by multiple peaks of kinetochore proteins in line scans through the spindle

Published October 20, 2014

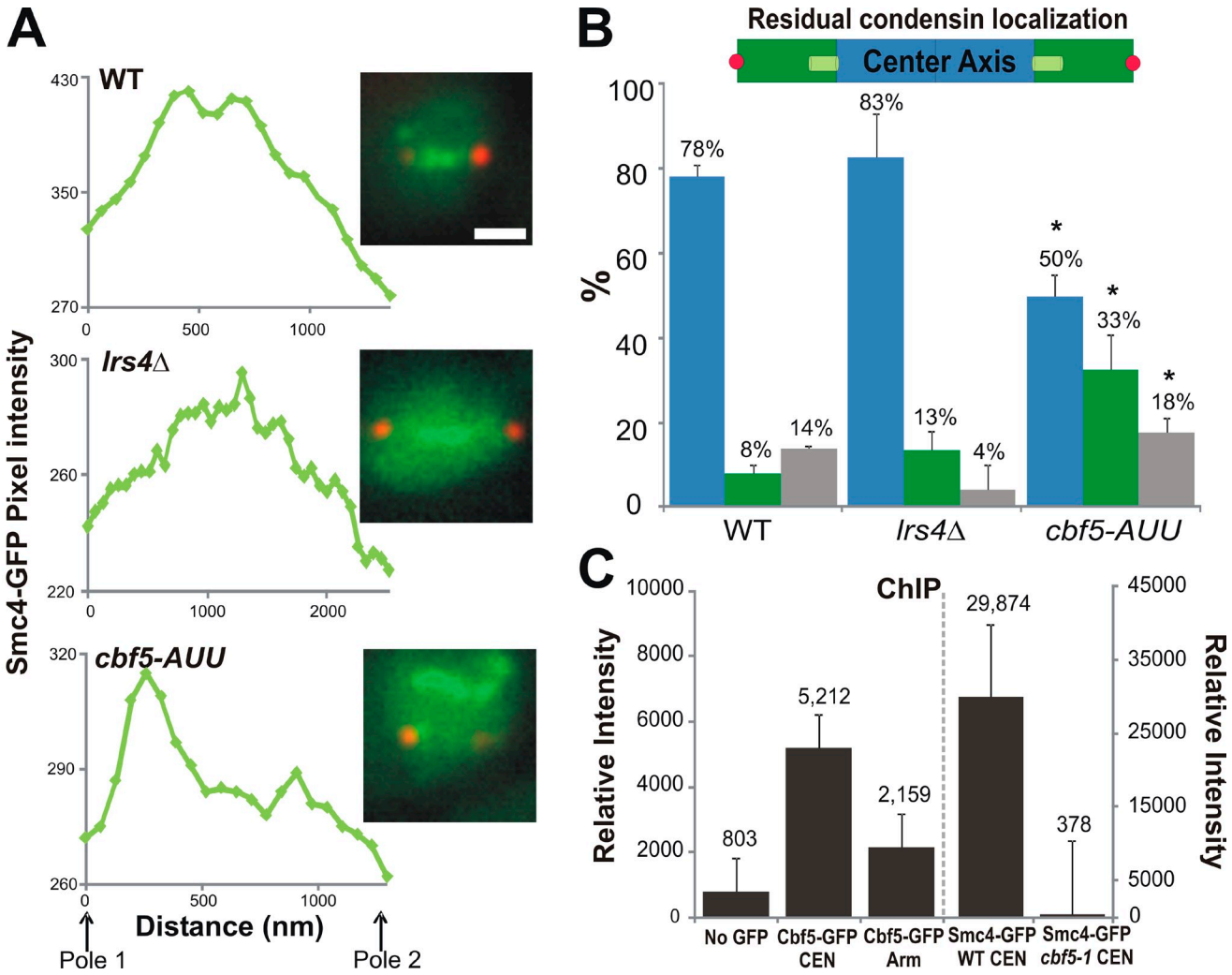

Figure 2. **Monopolin contributes to kinetochore-associated condensin, whereas Cbf5 contributes to condensin along the center of the spindle axis.** (A) Line scans were drawn through residual Smc4-GFP signal in WT, *lrs4Δ*, and *cbf5-1* mutants. Bar, 1 µm. (B) Residual condensin in *lrs4Δ* ($n = 22$) is predominantly localized to the central spindle axis, similar to WT ($n = 36$; $\chi^2 = 0.313$); in *cbf5-AUU*, the mutant ($n = 28$) displays an even distribution along the length of the spindle. The percentages of cells with peaks in both categories are represented by gray bars. Asterisks indicate a statistically significant change in distribution (*cbf5-AUU*; $\chi^2 = 7.84 \times 10^{-6}$); error bars represent standard deviation (two experiments). (C, left) Cbf5-GFP localizes to the centromere as determined by chromatin IP (ChIP). CEN3-associated Cbf5-GFP is sixfold more abundant than no GFP (six PCR trials) and approximately twofold more abundant than an arm locus (Htb1 locus; two PCR trials). (right) Smc4-GFP at centromere (WT-CEN) is significantly reduced upon shift of *cbf5-1* to restrictive temperature (37°C). The y axes denote Cbf5-GFP (left) and Smc4-GFP (right) relative intensity. Error bars show standard deviations.

axis; Fig. 3 B, Cse4-GFP in *lrs4Δ*) or exhibited a bilobed distribution in which the outer kinetochore is radially displaced from the spindle axis (Fig. 3 A, Nuf2-GFP in *lrs4Δ*, indicated by the decrease in fluorescence between the foci). Thus, dyskerin and monopolin are required for proper clustering and spindle proximal distribution of kinetochores.

We used model convolution and quantitative measurement of spindle structure to determine the basis for the bilobed distribution of kinetochore clusters in these mutants (Stephens et al., 2013b). Simulation of kinetochore microtubule plus ends arrayed cylindrically around the central spindle reveals that the bilobed pattern most likely reflects an increase in diameter of the cylindrical arrangement of kinetochore proteins around the spindle axis (Stephens et al., 2013b). To confirm this prediction, we measured the width of spindle kinetochore microtubule tufts labeled with tubulin-GFP to determine whether their diameter was increased. Tufts of 16 kinetochore microtubules were ~10% wider in the *cbf5-1* mutant (583 vs. 517 nm WT; Table 1). We estimate the increase in radius to be 50 nm in *cbf5-1* versus WT. The kinetochore is radially displaced as a result of a structural change of the pericentric chromatin, rather than direct alteration of the kinetochore. Thus, condensin recruitment through monopolin and dyskerin is integral to kinetochore structure (Fig. 3) and spindle length regulation (Table 1).

Condensin is required for sister chromatin biorientation along the spindle axis

To test whether condensin functions in sister chromatin biorientation, we examined the geometry of centromere-linked lactose operon (LacO) spots in metaphase. The LacO arrays generally appear as a single focus (Fig. 4 B, WT) but separate into two foci in longer spindles (Fig. 4 B; Pearson et al., 2001). Sister LacO arrays biorient along the spindle axis in both WT and cells depleted of pericentric cohesin (>98%; Fig. 4 A). In the

Published October 20, 2014

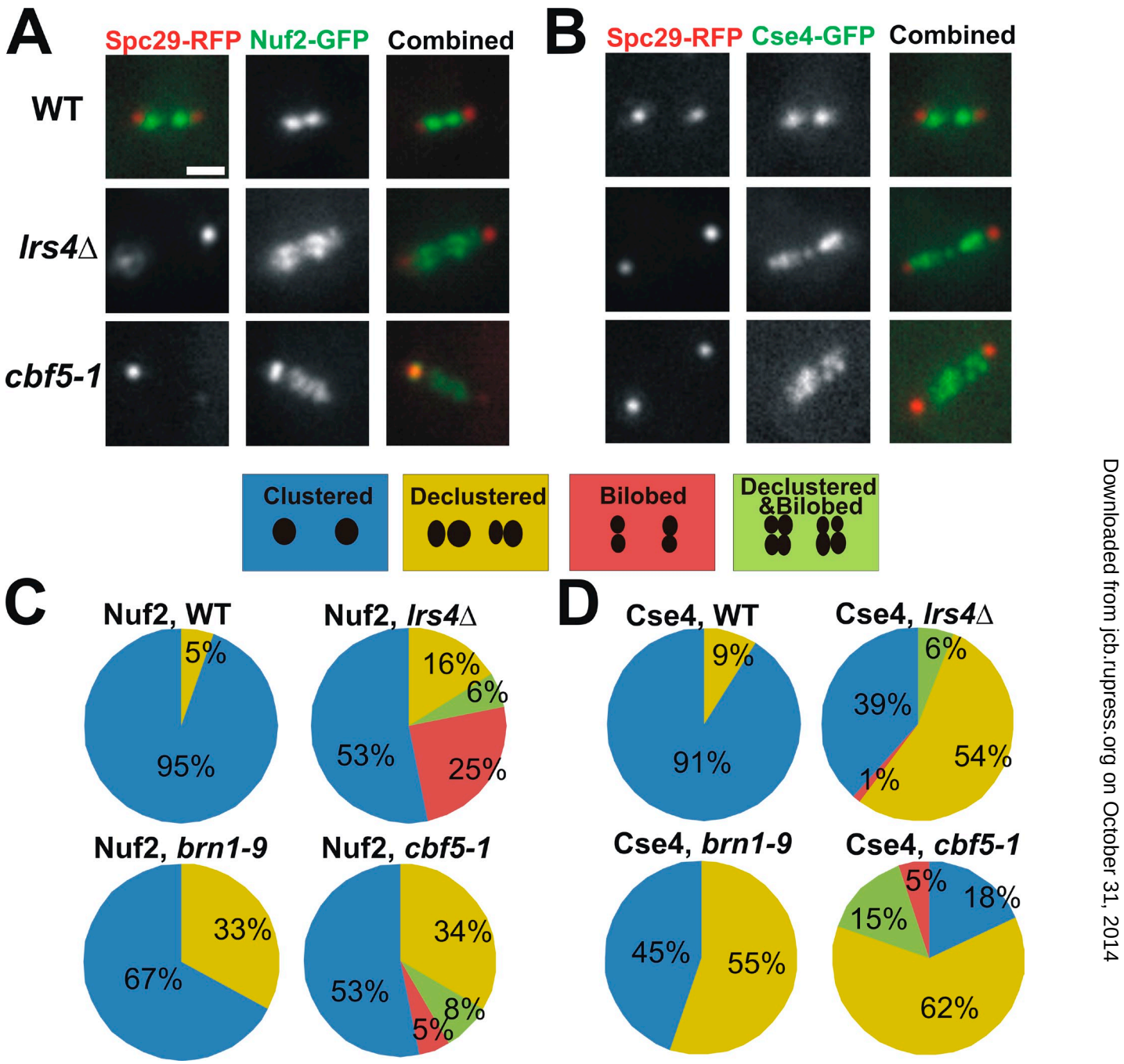

Figure 3. **Depletion of monopolin and Cbf5 disrupt kinetochore clustering.** (A and B) Kinetochore clusters (A, Nuf2; B, Cse4) are defined by a line scan drawn through the spindle axis (marked with Scp29-RFP). If there are greater than two peaks, the kinetochore is denoted as declustered. Bilobed refers to radial declustering of the kinetochore, as determined by two peaks on a line scan drawn perpendicular to the spindle axis through the kinetochore. (C and D) In *lrs4Δ* (Nuf2, $n = 148$; Cse4, $n = 81$) and *cbf5-1* (Nuf2, $n = 60$; Cse4, $n = 122$) mutants, both axial and radial declusterings of outer (C, Nuf2) and inner (D, Cse4) kinetochore components are observed ($\chi^2 < 1 \times 10^{-24}$). Bar, 1 µm.

absence of condensin (*brn1-9*), 27% of the LacO spots become misaligned and appear perpendicular to the spindle axis. Similarly, sister LacO arrays orient perpendicular to the spindle axis in 31% of cases in *cbf5-AUU* mutants and 23% of cases in monopolin mutants (Fig. 4 C). The separation between sister foci does not necessitate biorientation between kinetochore microtubules from opposite spindle poles. Recruitment to the microtubule spindle axis is dependent on the axial distribution of condensin, and Cbf5 plays a dominant role in this function.

Pericentric chromatin motion is perturbed in *cbf5-AUU* mutants

Pericentromeres of different chromosomes move coordinately in a condensin-dependent fashion (Stephens et al., 2013c). To determine whether dyskerin or monopolin was necessary for coordinated behavior, we imaged LacO and tetracycline operon (TetO) arrays linked to CEN15 and CEN11 (Fig. 4 D). These arrays were introduced into condensin (*brn1-9*), cohesin (*mcm21Δ*), dyskerin (*cbf5-AUU*), and monopolin (*lrs4Δ*) mutants

Published October 20, 2014

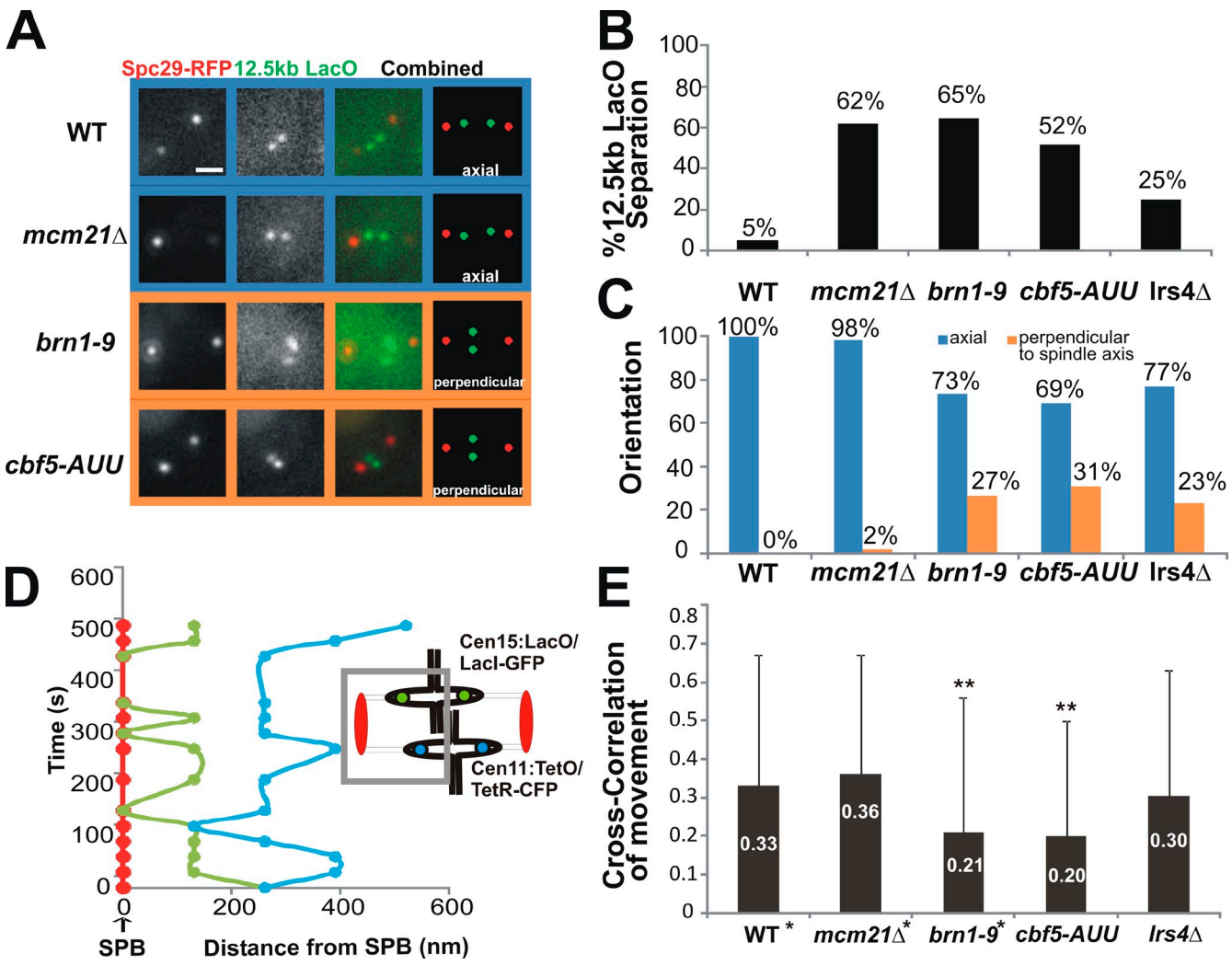

Figure 4. **Cbf5-dependent condensin is necessary for distribution of DNA along the spindle axis and for coordinated pericentromere motion.** (A) LacO arrays located 12.5 kb from CEN11 were analyzed in WT (n = 65, single experiment), *mcm21Δ* (n = 121), *brn1-9* (n = 88), and *cbf5-AUU* (n = 81) metaphase cells (defined by spindles 1.0–1.7 µm for WT; spindles ≤2.5 µm were included for mutants) and were classified by LacO separation. (B) 12.5-kb LacO is usually observed as one focus in WT but separates into two foci in longer spindles. (C) There was a significant increase in the perpendicular geometry of sister lacO arrays in *brn1-9* (n = 57) and *cbf5-AUU* (n = 42) mutants (WT, n = 33; *mcm21Δ*, n = 75). (D) Pericentromere movement tracked over time relative to Spc29-RFP using LacO (6.8 kb from CEN15) and TetO (4.5 kb from CEN11) fluorescent arrays. The graph represents motion of each array relative to the spindle pole in the half-spindle as shown in the schematic in one representative cell of the data in E. (E) Cross-correlation of pericentromere movement in metaphase for WT (n = 88), *mcm21Δ* (n = 54), *brn1-9* (n = 58), *cbf5-AUU* (n = 36), and *lrs4Δ* (n = 78). **, $P < 0.05$, t test. The single asterisks indicate that correlated motion data for WT, *mcm21Δ*, and *brn1-9* are from Stephens et al. (2013c). Error bars denote standard deviations. Bar, 1 µm.

(Fig. 4 E). The movements in the same half-spindle were compared using cross-correlation analysis (Stephens et al., 2013c). We find that correlated motion is decreased in the *cbf5-AUU* mutant to the same extent as found in *brn1-9* mutants (Fig. 4 E). In contrast, there is no significant reduction in correlated motion in *lrs4Δ* mutants in which condensin remains along the spindle axis (Fig. 4 E). Neither mutant decreased coordinated pericentromere stretching (Fig. S2 C). Thus, Cbf5-dependent condensin along the spindle axis is required for the behavior and coordination of pericentric chromatin motion in metaphase.

Role of pericentric tRNA genes in pericentric organization

To determine how pericentric tRNA genes promote coordinated movement between different pericentromeres, we analyzed Tfc1-GFP. In WT cells, Tfc1 localizes to the pericentromere between the poles in metaphase (Fig. 5 A). Like condensin, pericentric Tfc1 is heterogeneous and appears along the spindle or slightly displaced in ∼50% of cells (Fig. 5 A, images). To quantitate the distribution, we measured the width of a line scan through the axis perpendicular to the spindle. In WT cells, the peak-to-peak distance is 470 nm. There is a 20% increase in the peak-to-peak distance of the Tfc1 bilobed structure in the *cbf5-1* mutant (604 nm), indicative of radial expansion of Tfc1 localization. Thus, Cbf5 is necessary for maintenance of TFIIIC proximal to the spindle axis.

CBF5 could cluster condensin around the spindle axis in one of two ways. First, Cbf5 is reported to bind microtubules, which would present a viable mechanism for the axial positioning of condensin. Second, condensin could cross-link tRNA genes from different chromosomes. Based on the radial geometry of pericentric chromatin, cross-linking would gather strands

Published October 20, 2014

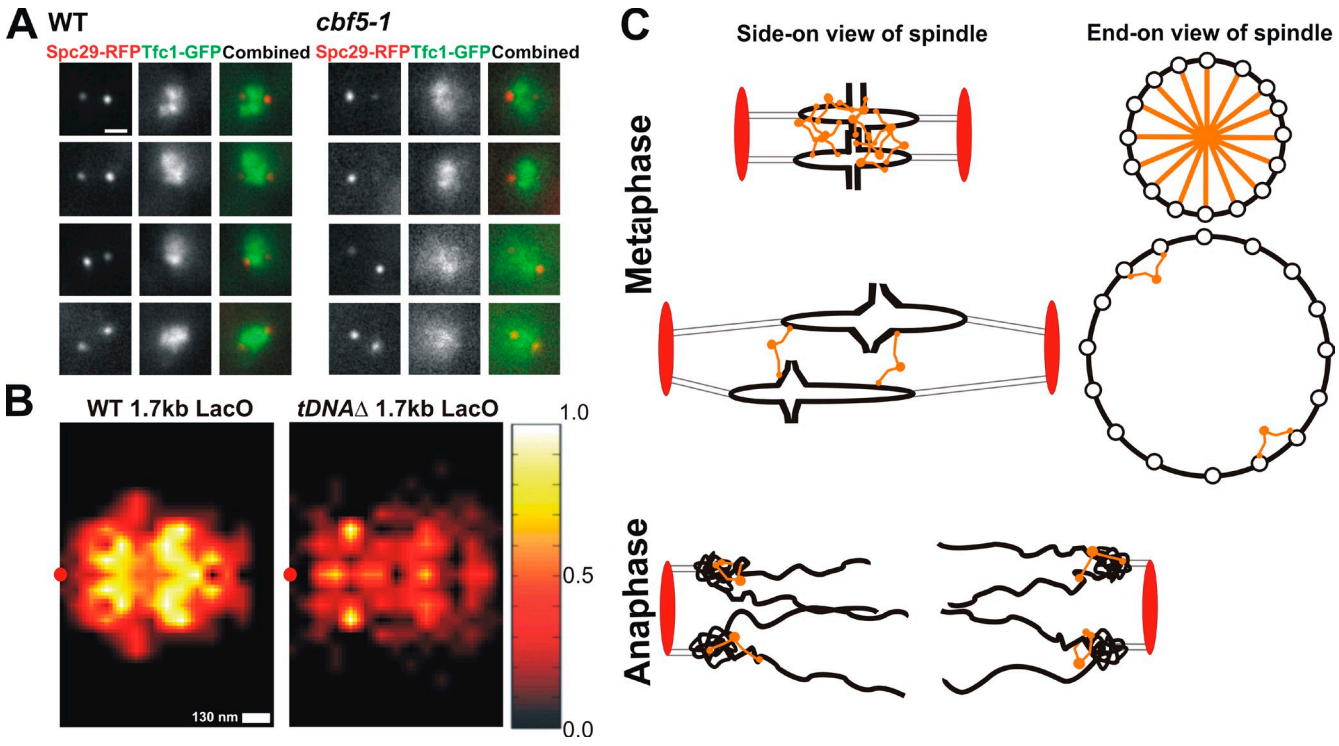

Figure 5. **Cbf5 and tRNA genes are required for spindle-proximal tethering of TFIIIC and pericentric chromatin, respectively.** (A, top) Tfc1 localizes to the metaphase spindle in WT and displays a bilobed phenotype in ∼50% of cells. Tfc1 displays greater peak-to-peak distance in *cbf5-1* mutants (n = 36) than in WT (n = 56), indicative of expansion from the spindle axis (470 nm ± 87 [WT] vs. 604 nm ± 99 [*cbf5-1*]; t test, $P < 0.05$). Bar, 1 µm. (B) The mean location of LacI-GFP bound to LacO in the presence or absence of tDNA was determined by measuring the distance of the LacO brightest pixel to the spindle pole body (red circles) in metaphase spindles. The statistical distribution of LacO is represented in heat maps for WT (n = 186) and *tDNAΔ* (n = 158) strains. The heat maps are color coded to represent number and position of the brightest pixel of the LacO foci relative to the pole (coordinates: 0,0) in both x (horizontal axis) and y (vertical axis). Areas in black are low probability, whereas yellow and white indicate areas of high probability. Without tDNA, LacO displays greater mean displacement from the spindle axis in y direction and greater distance from the spindle pole body in x direction. (C) Model for condensin and tDNA-mediated clustering of pericentromeres on the spindle axis. (top) Condensin associates with chromatin at tDNA sites and, through self-oligomerization, comes to lie along the spindle axis. (top right) In an end-on view of the spindle axis, condensin aggregation results in clustering of pericentromeres on the spindle axis. (middle) In the absence of tDNA, there is reduced condensin binding leading to a loss of aggregation and increased displacement from the spindle axis. The function of monopolin is indicated at the bottom. Monopolin is released from the nucleolus upon anaphase onset, in which it is predominantly localized to the quarter spindle closest to the spindle poles. This is consistent with its functional role in chromosome recoil during anaphase (Renshaw et al., 2010).

from different chromosomes to a central position. To distinguish these hypotheses, we deleted the C-terminal microtubule binding domain of Cbf5. Condensin intensity and distribution along the pericentric region was indistinguishable from WT (Fig. S1 B). If the transcription and modification enzymes function at the centromere-proximal tRNA genes, removal of the tRNA genes from one chromosome should lead to displacement of the pericentromere from the spindle axis. A strain was constructed in which all tDNA genes were removed from chromosome III with essential genes incorporated elsewhere in the genome. We analyzed the location of LacI-GFP bound to LacO in WT and the *tDNAΔ* strain. The LacO-GFP signal from individual cells is the same in WT and the tDNA delete strain.

Color-coded heat maps were created to represent the probability of LacO position relative to the spindle pole body (Fig. 5 B). The decrease in intensity reflects the change in distribution of LacO in WT versus *tDNAΔ* strains. The hot spots are reduced in the tDNA strain, indicating a reduced probability of localization of LacO. Furthermore, there is an increased radial displacement in *tDNAΔ*, indicative of increased randomness. In WT cells, the LacO position has a diameter of 240 ± 166 nm and a mean distance of 332 ± 200 nm from the spindle pole. Without tDNA on the LacO containing chromosome III, the diameter of LacO distribution expands to 271 ± 195 nm with a greater mean distance from the pole of 372 ± 234 nm (Table 2).

Cbf5 is enriched 1.5–3.5-fold across seven tDNAs on chromosome III as determined by chromatin IP–quantitative PCR (Fig. S3). Thus, tDNA contributes to pericentric chromatin organization by acting as a binding site for condensin, TFIIIC, and Cbf5. Together, the tRNA gene machinery promotes condensin localization to the spindle axis, therefore contributing to spindle-proximal constraint of pericentric chromatin.

Convergence of point and regional centromeres

The budding yeast centromere shares features with regional centromeres found in fission yeast *Schizosaccharomyces pombe* and perhaps multicellular eukaryotes. The major repeated DNA sequences in yeast are the rDNA, subtelomere repeats, long terminal repeats (LTRs; 300-400-bp bracketing retrotransposons, 429 total), and tDNA genes (307 total). LTRs and tDNA genes are enriched 1.8× in the 50-kb region surrounding the centromere, relative to the remainder of the genome. tRNA genes, as well as repeat elements, are enriched in fission yeast centromeres. In

Published October 20, 2014

Table 2. **Mean position of LacO 1.7 kb from CEN3 in WT and *tDNAΔ***

Strain	y displacement from spindle axis			Corrected distance in x between pole and LacO spot		Mean absolute LacO offset from spindle	*n*
	Mean	Total above and below	Standard deviation above and below	Mean	Standard deviation		
	nm	*nm*		*nm*		*nm*	
WT	119.80	239.70	166.07	331.79	200.28	167.57	186
tDNAΔ	135.30	270.68	195.36	372.28	233.69	184.81	158

Chironomus pallidivittatus, a SINE (short interspersed repeat) element, Cp1, is enriched in the centromeres (Rovira and Edström, 1996; Liao et al., 1998). Cp1 has a polymerase III box, typical of tRNA genes, and is found in the range of 5–10 copies per centromere (Liao et al., 1998). Repeat sequences and tRNA genes have been proposed to prevent heterochromatin spreading into the centromere (Donze et al., 1999; Scott et al., 2007; Raab et al., 2012) as well as contributing to heterochromatin clustering as loading sites for structural maintenance of chromosome proteins (Kirkland and Kamakaka, 2013). In this study, we identify a novel function for tRNA genes that form the basis for condensin's role in the chromatin spring.

The mechanism for restricting condensin to the spindle axis and repulsion of cohesin from the spindle axis had not been known. The enrichment of tRNA genes in the pericentric region led us to examine the role of tRNA transcription and modification factors as potential regulators. The transcription factor Tfc3 and modification enzyme, Cbf5 recruit condensin to the pericentromere and are responsible for the axial localization. Binding of tDNA transcription factor brings condensin proximal to the coding tDNA, which through aggregation of multiple tDNAs, results in the gathering of pericentromeres of different chromosomes. This will naturally lead to the centration of condensin along the spindle axis (Fig. 5 C). The removal of tDNA from chromosome III results in "puffing" of the pericentromere and an increase in the amount of space it can occupy (Fig. 5, B and C). The loss of tDNA results in the inability to secure the pericentromere of this chromosome to its neighbors, resulting in its expanded distance from the spindle axis.

The human homologue of Cbf5, dyskerin, functions in chromosome segregation fidelity in several organisms. Depletion of dyskerin results in mitotic defects, including delayed cell cycle progression, an increase in lagging chromosomes in anaphase, and activation of the spindle assembly checkpoint (Alawi and Lin, 2013). Upon depletion of *cbf5-1* in budding yeast, we witness perturbation of kinetochore clustering and an increase in spindle length. We attribute these defects to a disruption of the pericentromere caused by loss of condensin along the spindle axis. A characteristic of mammalian cells depleted of condensin is the loss of ability of the kinetochore to sense tension (Ribeiro et al., 2009), metaphase arrest, and missegregation of chromosomes when the spindle checkpoint is inactivated (Yong-Gonzalez et al., 2007). Thus, mitotic dyskerin phenotypes in mammalian cells may be a consequence of reduced condensin levels within the spindle.

We propose that the functional consequence of condensin and Cbf5 binding to TFIIIC sites in tRNA genes is the building of a chromosome tether. A major mechanism for regulating chromosome dynamics is through tethering the centromere to a spindle pole or telomeres to the nuclear envelope (Verdaasdonk et al., 2013). Our tenet is that tethers throughout the chromosome dictate local dynamics that facilitate or restrict movement optimal for a given DNA metabolic process, such as DNA repair or mitotic force balance. In the pericentromere, the tethers are critical for force balance. It is currently thought that cohesin, by promoting sister chromatid cohesion is the basis for resisting microtubule forces from opposite spindle poles. However, pericentric cohesin is radially displaced from the spindle axis and therefore mechanically decoupled from direct microtubule-based force. In contrast, condensin is colinear with the kinetochore microtubules and likely to be involved in this process. The finding herein provides a mechanism for how the extensional forces are resisted. Condensin is cross-linked to different chromosomes to resist extensional forces through the network.

This provides a framework for integrating several recent findings regarding the distribution of TFIIIC binding sites. Incomplete TFIIIC sites are found throughout the genome (Moqtaderi et al., 2010). Condensin recruitment to these sites via Tfc3 could act in a similar fashion as condensin bound to tRNA genes in the pericentromere and for topological chromatin domains in *Drosophila melanogaster* (Van Bortle et al., 2014).

Upon anaphase onset, cohesin is degraded, and the pericentric chromatin rapidly migrates to the pole. Condensin is no longer required for force balance at this juncture. Instead, condensin has been shown to facilitate the recoil of chromosome arms to the spindle poles (Renshaw et al., 2010). This function is temporally correlated with the release of monopolin from the nucleolus. Monopolin is situated in a pole proximal position (Fig. 2), where its role in chromosome condensation is commensurate with a biological role in anaphase compaction (Fig. 5 C). Condensin's critical role in the mitotic spindle is thus spatially and temporally partitioned by dyskerin for force balance in metaphase and monopolin for compaction in anaphase.

Materials and methods

Cell preparation

Cells were grown in YPD media (2% glucose, 2% peptone, and 1% yeast extract) at 24°C for WT, *lrs4Δ*, and *cbf5-AUU* strains. Temperature-sensitive strains (*cbf5-1* and *tfc3-tsv115*) were grown at 24°C and then shifted to 37°C 6 h before imaging. Temperature-sensitive strains containing *cbf5-1* were provided by J. Carbon (University of California, Santa Barbara, Santa Barbara, CA), and *tfc3-tsv115* was given by F. Uhlmann (London Research Institute, London, England, UK).

Microscopy

Images were acquired with a microscope stand (Eclipse TE2000-U; Nikon) with a 100× Plan Apochromat, 1.4 NA 100× digital interference contrast

Published October 20, 2014

oil immersion lens with a camera (ORCA-ER; Hamamatsu Photonics) at room temperature (25°C). MetaMorph 7.1 (Molecular Devices) was used to acquire unbinned images of in a seven-step z series with a 300-nm step size of Smc4-GFP, kinetochore proteins Nuf2-GFP and Cse4-2×GFP, 12.5-kb LacO, Tfc1-GFP, Cbf5-GFP, and Lrs4-GFP. Images were taken with 600-ms exposure times for RFP and GFP in water on 0.135-mm coverslips. Images of 1.7-kb LacO arrays in *tDNAΔ* and WT were acquired in 10 200-nm steps. Population images of the CEN15 LacO/LacI-GFP and CEN11 TetO/TetR-CFP strain were binned 2× and acquired in 10 200-nm steps, whereas time-lapse images were acquired in single planes at 15- and 30-s time intervals. Live cells were imaged in synthetic growth medium.

Fluorescent constructs and mutations

Smc4-GFP is a GFP fusion to the C-terminal amino acid of the Smc4 subunit of condensin, and Spc29-RFP is a RFP fusion to the C-terminal amino acid of the spindle pole protein Spc29 (Stephens et al., 2011). Nuf2-GFP, Cbf5-GFP, Lrs4-GFP, and Tfc1-GFP are GFP fusions to the C-terminal codons of the respective genes using the GFP-MX6 plasmids described in Wach et al. (1997). Cdc14-CFP is a CFP fusion to the C terminus of *CDC14*. Cse4-2×GFP contains tandem copies of GFP inserted at amino acid position 83 of Cse4 (pRB920). The CBF5 C-terminal truncation was a 40–amino acid truncation that removes 7/10 of the terminal KKD/E repeats within the Cbf5 protein. The construct supports growth and exhibits <1% the microtubule-binding activity determined by Jiang et al. (1993).

The GAL1-regulated control of Nop10 and Nhp2 gene expression was constructed with the promoter substitution cassettes described by Janke et al. (2004). A truncated (weaker) GAL1 promoter, denoted GALL, was inserted upstream from the ATG of Nop10 and Nhp2. Cell growth was supported on galactose and not on glucose. LacI-GFP is a fusion protein of GFP-LacI-NLS driven by the *HIS3* promoter, with the LacI gene deleted for 11 C-terminal amino acids to prevent tetramerization (Straight et al., 1996). TetR-CFP is a full-length fusion of TetR to CFP, driven by the *URA3* promoter (Bressan et al., 2004). The binding sites for these fusions, LacO and TetO arrays, are tandem copies of the operator sequence constructed from a LacO 8-mer on a 292-bp sequence as described by Robinett et al. (1996). The number of arrays and position in the genome are indicated in the section LacO array analysis.

Analysis of Smc4 fluorescence

Images of Smc4-GFP were aligned horizontally with regards to the spindle axis (determined by Spc29-RFP) using MATLAB (MathWorks, Inc.). The integrated intensity of Smc4 along the spindle was determined by centering a 37 × 11–pixel rectangle (inner region) over the spindle and then centering a 47 × 21–pixel rectangle (outer region) over the inner region and logging the integrated intensity of both regions to Excel (Microsoft) using MetaMorph. Integrated intensity of Smc4 (F_{Smc4}) was then determined by the following formula: $F_{Smc4} = F_I - F_{background}$, in which $F_{background} = (F_O - F_I) \times$ (area of inner region − area between perimeter of inner and outer regions), F_I = integrated intensity of inner region, and F_O = integrated intensity of outer region.

Localization of residual Smc4 was determined by drawing line scans with a height of one pixel and width long enough to span the spindle length of horizontally aligned images with respect to the spindle axis. Line scans drawn in MetaMorph 7.1 were then logged to Excel and graphed as a function of pixel intensity versus spindle length. The length of the spindle was then divided into four quadrants. Localization was determined as at the pole if any line scan peaks occurred in the outer two quadrants, whereas peaks occurring in the two inner quadrants were classified as center of the axis.

For determination of Smc4-GFP position within the spindle (Fig. 2 B), the spindle (determined by Spc29-RFP) was divided into four quadrants, with the outer two quadrants representing the kinetochore and spindle pole region (Fig. 2 B, green) and the inner two quadrants representing the center zone of the spindle (Fig. 2 B, blue). Peaks falling within the two inner quadrants were classified as within the middle 50% of spindle length, whereas peaks falling within the outer two quadrants were classified as within <25% or >75% of spindle length (localized to the kinetochore and spindle pole region).

Chromatin IP

Cells were grown to an OD_{660} of 0.4 in YPD. HCHO was added to a final concentration of 1% for 20 min at room temperature followed by the adding of glycine to a final concentration of 125 mM. Pellets were resuspended in FA (fixation)-lysis buffer (50 mM Hepes-KOH, pH 7.5, 300 mM NaCl, 1 mM EDTA, 1% Triton X-100, 0.1% sodium deoxycholate, and protease inhibitor cocktail) and vortexed with acid-washed glass beads for 1 h at 4°C. After sonication of the lysate, protein concentration of the whole cell extract was assayed using the protein assay kit (Dye Reagent Concentrate; Bio-Rad Laboratories). For IP reactions, whole cell extract was added to make final protein concentration 3 mg with 12 µl anti-GFP rabbit IgG fraction antibody (Life Technologies) and FA-lysis buffer to bring the final volume to 500 µl. IP reactions were allowed to rock at 4°C overnight before 12 µl FA-lysis buffer–washed Dynabeads Protein A (Life Technologies) was added to each IP and allowed to rock an additional 3 h. Antigens were eluted from the beads with 1% SDS and 0.1 M $NaHCO_3$ after sequential washing of the beads with FA-lysis buffer, FA-lysis buffer with 500 mM NaCl, LiCl solution, TE (10 mM Tris-HCl and 1 mM EDTA, pH 8.0), pH 8.0, and TE, pH 8.0, containing 20 µg RNase A. 16 µl of 5-M NaCl was added to eluate and input samples and allowed to incubate at 65°C overnight to reverse cross-links. DNA purification was completed using the PCR purification kit protocol (QIAquick; QIAGEN). PCR was used to analyze the purified DNA. Oligonucleotides for CEN span a 625-bp region of CENIII (up: 5′-GATCAGCGCCAAACAATATGG-3′; down: 5′-GGGTGGGAAACTGAAGAAATC-3′). Oligonucleotides for arm span a 920-bp region of Htb1 (up: 5′-CTACCTTGGTTGGTTATCTTGTAACGATTGGTAAG-3′; down: 5′-GAAAAATCTAGTATTGTTCACACGAGCCAATGCTCTG-3′). PCR products run on 1% agarose gels were analyzed using MetaMorph 7.1. Integrated intensity of the bands on the gel was analyzed by drawing a rectangle to fit the band on the gel and a second rectangle around the first. Intensity was then calculated using the following formula: $F_{band} = F_I - F_{background}$, in which $F_{background} = (F_O - F_I) \times$ (area of inner region − area between perimeter of inner and outer regions), F_I = integrated intensity of inner region, and F_O = integrated intensity of outer region.

Kinetochore declustering and Tfc1 analysis

Population images were taken of Spc29-RFP and GFP-tagged kinetochore components (Nuf2-GFP and Cse4-2×GFP). Cse4-2×GFP was provided by R. Baker (University of Massachusetts Medical School, Worcester, MA). Using MetaMorph 7.1, line scans were drawn through each sister kinetochore along the spindle axis (axial) or perpendicular to the spindle axis (radial) to determine whether the kinetochore was clustered (one peak) or declustered (multiple peaks). Similarly, population images of Tfc1-GFP and Spc29-RFP were rotated and aligned relative to the spindle axis using MATLAB. Line scans drawn through Tfc1 signal perpendicular to the spindle axis were used to determine inclusive peak-to-peak measurements.

LacO array analysis

Population images of metaphase cells were acquired of strains with 12.5-kb LacO arrays in WT, GalH3, *mcm21Δ*, *brn1-9*, and *cbf5-AUU* mutants. Orientation relative to the spindle axis was determined as axial if both foci lie parallel to the spindle axis, whereas perpendicular orientation was determined by foci lying at a 90° angle to the axis. The 12.5-kb LacO array is a 32-mer repeat of the Lac operator (1.2 kb in length) introduced 12.7 kb from the centromere on chromosome XI (Pearson et al., 2001). The coordinates relative to CEN11 (440,246–440,129) are 427,362–427,412 on chromosome XI.

To determine cross-correlation of pericentric movement (Fig. 4, D and E), strains containing a 10-kb LacO/LacI-GFP 1.8 kb from CEN15 (centroid of 6.8 kb; Goshima and Yanagida, 2000), 8-kb TetO/TetR CFP 0.4 kb from CEN11 (centroid of 4.5 kb), and Spc29-RFP were built (Stephens et al., 2013c). The TetO arrays were amplified from the plasmid backbone described in Rohner et al. (2008). The coordinates relative to CEN11 (440,246–440,129) were 439,644–439,412 on chromosome XI. Images were acquired in single planes (binned 2×) over time at 15- or 30-s intervals. Each image at every time point was aligned horizontally with regard to the spindle axis using Spc29-RFP. Distance in nanometers (x axis) from LacO and TetO to the pole was measured at each time point, and correlation of these distances over time was calculated using the CORREL function in Excel.

Coordinated stretching was measured using the strain described in the previous paragraph by taking population images in 10 200-nm z steps (binned 2×). Stretching events were determined as one focus and another linear fluorescent signal (aspect ratio > 1.2). Stretching events were defined as uncoordinated if one array (either LacO or TetO) is stretched in any given cell and coordinated if both arrays are stretched.

For heat mapping, images of 1.7-kb LacO/LacI-GFP were rotated and aligned relative to the spindle axis (determined by Spc29-RFP) using MATLAB. The LacO array is a 1.2-kb 32-mer described in LacO array analysis, inserted at Met14 1.1 kb from the centromere on chromosome XI (Pearson et al., 2001). The distance in x and y from the spindle pole was measured for the brightest pixel of each LacO and logged in Excel. The number of occurrences of a LacO occupying a position within one quadrant of the spindle was recorded and mirrored across the x axis.

This information was transferred to MATLAB, in which an image was generated using the black body radiation spectrum to depict probability of the LacO position.

Online supplemental material

Fig. S1 shows that box H/ACA snoRNP complex members are necessary for condensin enrichment at the pericentromere. Fig. S2 shows localization and function of Cbf5 and monopolin. Fig. S3 shows the concentration of CBF5-GFP determined by chromatin IP at sites of the genome where the tRNA genes on chromosome III were deleted. Table S1 provides a list of the strains used in this study. Online supplemental material is available at http://www.jcb.org/cgi/content/full/jcb.201405028/DC1.

The authors thank members of the Bloom laboratory for critical reading of the manuscript. We thank Mr. Jiasheng (David) Guo for technical assistance, Dr. John Carbon for strain YHY64a1 containing the *cbf5-1* mutation, Dr. Richard Baker for plasmid pRB920 containing Cse4-2×GFP, and Dr. Frank Uhlmann for strain Y3339 containing the *tfc3-tsv115* mutation.

This work was supported by grants R37 GM32238 to K. Bloom, GM078068 to R.T. Kamakaka, and T32-GM008646 to J.G. Kirkland and O. Hamdani.

The authors declare no competing financial interests.

Submitted: 8 May 2014
Accepted: 9 September 2014

References

Alawi, F., and P. Lin. 2013. Dyskerin localizes to the mitotic apparatus and is required for orderly mitosis in human cells. *PLoS ONE*. 8:e80805. http://dx.doi.org/10.1371/journal.pone.0080805

Blat, Y., and N. Kleckner. 1999. Cohesins bind to preferential sites along yeast chromosome III, with differential regulation along arms versus the centric region. *Cell*. 98:249–259. http://dx.doi.org/10.1016/S0092-8674(00)81019-3

Bressan, D.A., J. Vazquez, and J.E. Haber. 2004. Mating type–dependent constraints on the mobility of the left arm of yeast chromosome III. *J. Cell Biol.* 164:361–371. http://dx.doi.org/10.1083/jcb.200311063

Brito, I.L., F. Monje-Casas, and A. Amon. 2010. The Lrs4-Csm1 monopolin complex associates with kinetochores during anaphase and is required for accurate chromosome segregation. *Cell Cycle*. 9:3611–3618. http://dx.doi.org/10.4161/cc.9.17.12885

Burrack, L.S., S.E. Applen Clancey, J.M. Chacón, M.K. Gardner, and J. Berman. 2013. Monopolin recruits condensin to organize centromere DNA and repetitive DNA sequences. *Mol. Biol. Cell*. 24:2807–2819. http://dx.doi.org/10.1091/mbc.E13-05-0229

D'Ambrosio, C., C.K. Schmidt, Y. Katou, G. Kelly, T. Itoh, K. Shirahige, and F. Uhlmann. 2008. Identification of cis-acting sites for condensin loading onto budding yeast chromosomes. *Genes Dev.* 22:2215–2227. http://dx.doi.org/10.1101/gad.1675708

Donze, D., C.R. Adams, J. Rine, and R.T. Kamakaka. 1999. The boundaries of the silenced HMR domain in *Saccharomyces cerevisiae*. *Genes Dev.* 13:698–708. http://dx.doi.org/10.1101/gad.13.6.698

Gardano, L., L. Holland, R. Oulton, T. Le Bihan, and L. Harrington. 2012. Native gel electrophoresis of human telomerase distinguishes active complexes with or without dyskerin. *Nucleic Acids Res.* 40:e36. http://dx.doi.org/10.1093/nar/gkr1243

Goshima, G., and M. Yanagida. 2000. Establishing biorientation occurs with precocious separation of the sister kinetochores, but not the arms, in the early spindle of budding yeast. *Cell*. 100:619–633. http://dx.doi.org/10.1016/S0092-8674(00)80699-6

Gu, B., M. Bessler, and P.J. Mason. 2009. Dyskerin, telomerase and the DNA damage response. *Cell Cycle*. 8:6–10. http://dx.doi.org/10.4161/cc.8.1.7265

Haeusler, R.A., M. Pratt-Hyatt, P.D. Good, T.A. Gipson, and D.R. Engelke. 2008. Clustering of yeast tRNA genes is mediated by specific association of condensin with tRNA gene transcription complexes. *Genes Dev.* 22:2204–2214. http://dx.doi.org/10.1101/gad.1675908

Hirano, T. 2006. At the heart of the chromosome: SMC proteins in action. *Nat. Rev. Mol. Cell Biol.* 7:311–322. http://dx.doi.org/10.1038/nrm1909

Hoang, C., and A.R. Ferré-D'Amaré. 2001. Cocrystal structure of a tRNA Psi55 pseudouridine synthase: nucleotide flipping by an RNA-modifying enzyme. *Cell*. 107:929–939. http://dx.doi.org/10.1016/S0092-8674(01)00618-3

Iwasaki, O., and K. Noma. 2012. Global genome organization mediated by RNA polymerase III-transcribed genes in fission yeast. *Gene*. 493:195–200. http://dx.doi.org/10.1016/j.gene.2010.12.011

Janke, C., M.M. Magiera, N. Rathfelder, C. Taxis, S. Reber, H. Maekawa, A. Moreno-Borchart, G. Doenges, E. Schwob, E. Schiebel, and M. Knop. 2004. A versatile toolbox for PCR-based tagging of yeast genes: new fluorescent proteins, more markers and promoter substitution cassettes. *Yeast*. 21:947–962. http://dx.doi.org/10.1002/yea.1142

Jiang, W., K. Middleton, H.J. Yoon, C. Fouquet, and J. Carbon. 1993. An essential yeast protein, CBF5p, binds in vitro to centromeres and microtubules. *Mol. Cell. Biol.* 13:4884–4893.

Kendall, A., M.W. Hull, E. Bertrand, P.D. Good, R.H. Singer, and D.R. Engelke. 2000. A CBF5 mutation that disrupts nucleolar localization of early tRNA biosynthesis in yeast also suppresses tRNA gene-mediated transcriptional silencing. *Proc. Natl. Acad. Sci. USA*. 97:13108–13113. http://dx.doi.org/10.1073/pnas.240454997

Kirkland, J.G., and R.T. Kamakaka. 2013. Long-range heterochromatin association is mediated by silencing and double-strand DNA break repair proteins. *J. Cell Biol.* 201:809–826. http://dx.doi.org/10.1083/jcb.201211105

Kuhn, R.M., L. Clarke, and J. Carbon. 1991. Clustered tRNA genes in *Schizosaccharomyces pombe* centromeric DNA sequence repeats. *Proc. Natl. Acad. Sci. USA*. 88:1306–1310. http://dx.doi.org/10.1073/pnas.88.4.1306

Liao, C., C. Rovira, H. He, and J.E. Edström. 1998. Site-specific insertion of a SINE-like element, Cp1, into centromeric tandem repeats from *Chironomus pallidivittatus*. *J. Mol. Biol.* 280:811–820. http://dx.doi.org/10.1006/jmbi.1998.1896

Megee, P.C., C. Mistrot, V. Guacci, and D. Koshland. 1999. The centromeric sister chromatid cohesion site directs Mcd1p binding to adjacent sequences. *Mol. Cell*. 4:445–450. http://dx.doi.org/10.1016/S1097-2765(00)80347-0

Moqtaderi, Z., J. Wang, D. Raha, R.J. White, M. Snyder, Z. Weng, and K. Struhl. 2010. Genomic binding profiles of functionally distinct RNA polymerase III transcription complexes in human cells. *Nat. Struct. Mol. Biol.* 17:635–640. http://dx.doi.org/10.1038/nsmb.1794

Mumberg, D., R. Müller, and M. Funk. 1994. Regulatable promoters of *Saccharomyces cerevisiae*: comparison of transcriptional activity and their use for heterologous expression. *Nucleic Acids Res.* 22:5767–5768. http://dx.doi.org/10.1093/nar/22.25.5767

Pearson, C.G., P.S. Maddox, E.D. Salmon, and K. Bloom. 2001. Budding yeast chromosome structure and dynamics during mitosis. *J. Cell Biol.* 152:1255–1266. http://dx.doi.org/10.1083/jcb.152.6.1255

Raab, J.R., J. Chiu, J. Zhu, S. Katzman, S. Kurukuti, P.A. Wade, D. Haussler, and R.T. Kamakaka. 2012. Human tRNA genes function as chromatin insulators. *EMBO J.* 31:330–350. http://dx.doi.org/10.1038/emboj.2011.406

Renshaw, M.J., J.J. Ward, M. Kanemaki, K. Natsume, F.J. Nédélec, and T.U. Tanaka. 2010. Condensins promote chromosome recoiling during early anaphase to complete sister chromatid separation. *Dev. Cell*. 19:232–244. http://dx.doi.org/10.1016/j.devcel.2010.07.013

Ribeiro, S.A., J.C. Gatlin, Y. Dong, A. Joglekar, L. Cameron, D.F. Hudson, C.J. Farr, B.F. McEwen, E.D. Salmon, W.C. Earnshaw, and P. Vagnarelli. 2009. Condensin regulates the stiffness of vertebrate centromeres. *Mol. Biol. Cell*. 20:2371–2380. http://dx.doi.org/10.1091/mbc.E08-11-1127

Robinett, C.C., A. Straight, G. Li, C. Willhelm, G. Sudlow, A. Murray, and A.S. Belmont. 1996. In vivo localization of DNA sequences and visualization of large-scale chromatin organization using lac operator/repressor recognition. *J. Cell Biol.* 135:1685–1700. http://dx.doi.org/10.1083/jcb.135.6.1685

Rohner, S., S.M. Gasser, and P. Meister. 2008. Modules for cloning-free chromatin tagging in *Saccharomyces cerevisiae*. *Yeast*. 25:235–239. http://dx.doi.org/10.1002/yea.1580

Rovira, C., and J.E. Edström. 1996. Centromeric polymerase III transcription units in *Chironomus pallidivittatus*. *Nucleic Acids Res.* 24:1662–1668. http://dx.doi.org/10.1093/nar/24.9.1662

Scott, K.C., C.V. White, and H.F. Willard. 2007. An RNA polymerase III-dependent heterochromatin barrier at fission yeast centromere 1. *PLoS ONE*. 2:e1099. http://dx.doi.org/10.1371/journal.pone.0001099

Stephens, A.D., J. Haase, L. Vicci, R.M. Taylor II, and K. Bloom. 2011. Cohesin, condensin, and the intramolecular centromere loop together generate the mitotic chromatin spring. *J. Cell Biol.* 193:1167–1180. http://dx.doi.org/10.1083/jcb.201103138

Stephens, A.D., R.A. Haggerty, P.A. Vasquez, L. Vicci, C.E. Snider, F. Shi, C. Quammen, C. Mullins, J. Haase, R.M. Taylor II, et al. 2013a. Pericentric chromatin loops function as a nonlinear spring in mitotic force balance. *J. Cell Biol.* 200:757–772. http://dx.doi.org/10.1083/jcb.201208163

Stephens, A.D., C.W. Quammen, B. Chang, J. Haase, R.M. Taylor II, and K. Bloom. 2013b. The spatial segregation of pericentric cohesin and condensin in the mitotic spindle. *Mol. Biol. Cell*. 24:3909–3919. http://dx.doi.org/10.1091/mbc.E13-06-0325

Stephens, A.D., C.E. Snider, J. Haase, R.A. Haggerty, P.A. Vasquez, M.G. Forest, and K. Bloom. 2013c. Individual pericentromeres display coordinated motion and stretching in the yeast spindle. *J. Cell Biol.* 203:407–416. http://dx.doi.org/10.1083/jcb.201307104

Straight, A.F., A.S. Belmont, C.C. Robinett, and A.W. Murray. 1996. GFP tagging of budding yeast chromosomes reveals that protein-protein interactions can mediate sister chromatid cohesion. *Curr. Biol.* 6:1599–1608. http://dx.doi.org/10.1016/S0960-9822(02)70783-5

Van Bortle, K., M.H. Nichols, L. Li, C.T. Ong, N. Takenaka, Z.S. Qin, and V.G. Corces. 2014. Insulator function and topological domain border strength scale with architectural protein occupancy. *Genome Biol.* 15:R82. http://dx.doi.org/10.1186/gb-2014-15-5-r82

Verdaasdonk, J.S., P.A. Vasquez, R.M. Barry, T. Barry, S. Goodwin, M.G. Forest, and K. Bloom. 2013. Centromere tethering confines chromosome domains. *Mol. Cell*. 52:819–831. http://dx.doi.org/10.1016/j.molcel.2013.10.021

Wach, A., A. Brachat, C. Alberti-Segui, C. Rebischung, and P. Philippsen. 1997. Heterologous HIS3 marker and GFP reporter modules for PCR-targeting in *Saccharomyces cerevisiae. Yeast.* 13:1065–1075. http://dx.doi.org/10.1002/(SICI)1097-0061(19970915)13:11<1065::AID-YEA159>3.0.CO;2-K

Yong-Gonzalez, V., B.D. Wang, P. Butylin, I. Ouspenski, and A. Strunnikov. 2007. Condensin function at centromere chromatin facilitates proper kinetochore tension and ensures correct mitotic segregation of sister chromatids. *Genes Cells*. 12:1075–1090. http://dx.doi.org/10.1111/j.1365-2443.2007.01109.x

Snider et al., http://www.jcb.org/cgi/content/full/jcb.201405028/DC1

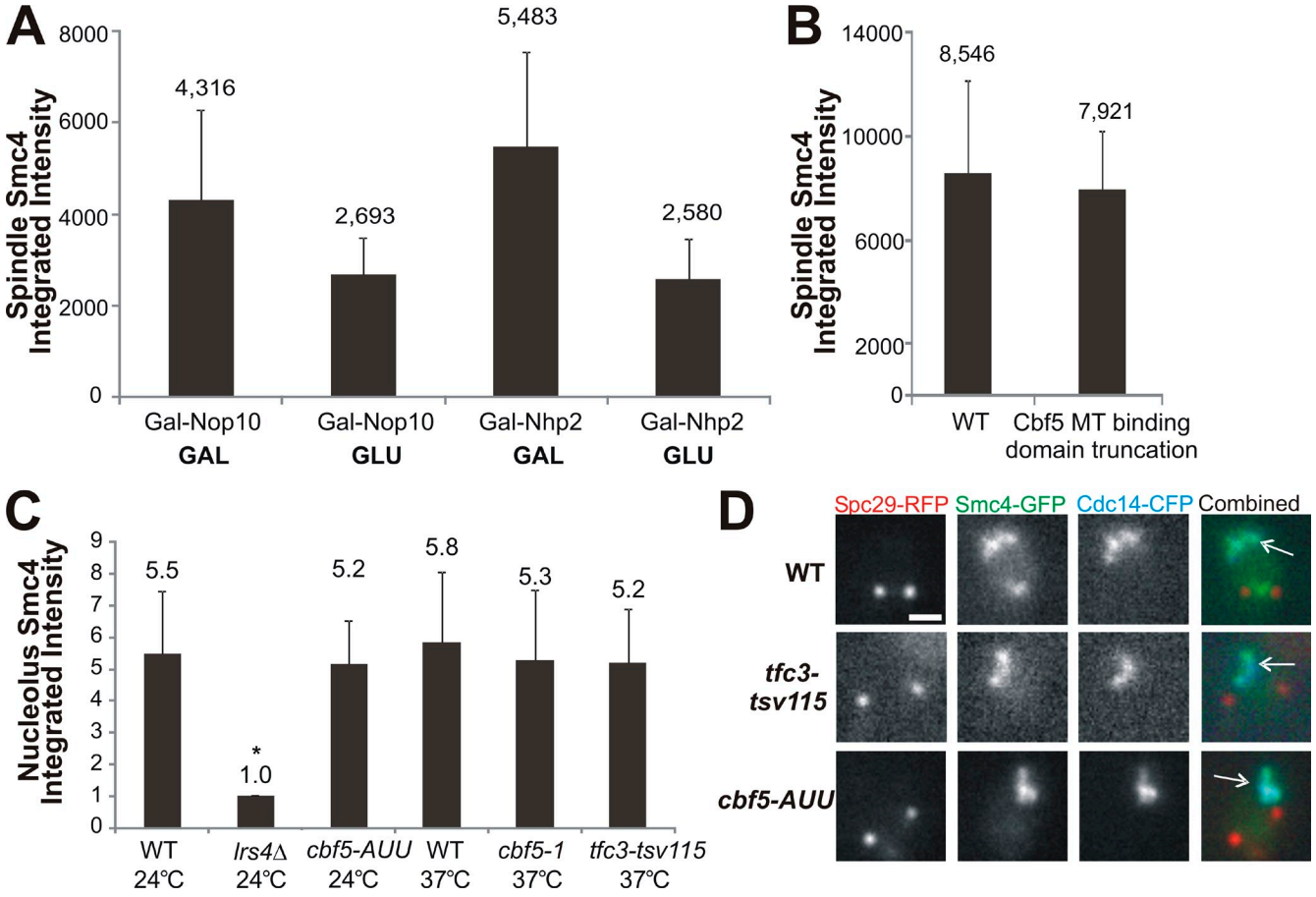

Figure S1. **Box H/ACA snoRNP complex members are necessary for condensin enrichment at the pericentromere.** (A) Smc4-GFP was analyzed in strains with Nop10 and Nhp2 under GAL1 promoters in metaphase cells in both galactose (GAL1-Nop10, $n = 25$; GAL1-Nhp2, $n = 12$) and after 4 h of growth in glucose (GAL1-Nop10, $n = 22$; GAL1-Nhp2, $n = 36$). Significant drops in spindle Smc4 intensity were observed after growth on glucose, indicating that perhaps Cbf5, Nop10, and Nhp2 work together as a complex to bring condensin to the spindle axis in metaphase. GAL, growth on galactose; GLU, growth on glucose. (B) Smc4-GFP was imaged with Spc29-RFP in WT cells and in a mutant with a truncation of the microtubule binding domain of Cbf5. Integrated intensity of Smc4-GFP was measured between the poles ($n = 32$) but did not display a significant drop from WT Smc4 levels (*t* test, $P = 0.4$). (C) Integrated intensity of Smc4-GFP was measured at the rDNA locus (indicated by arrows in Fig. 1 example images) in metaphase cells and reported as a ratio of pericentric intensity/nuclear intensity at 24°C for WT ($n = 50$), *lrs4Δ* ($n = 93$), and *cbf5-AUU* ($n = 14$). WT ($n = 67$) and temperature-sensitive mutants *cbf5-1* ($n = 80$) and *tfc3-tsv115* ($n = 46$) were analyzed after 6 h at restrictive temperature (37°C). Asterisk denotes a statistically significant difference from WT (*t* test, $P < 0.05$). Error bars represent standard deviations. (D) Smc4-GFP was imaged with Cdc14-CFP and Spc29-RFP in WT, *tfc3-tsv115*, and *cbf5-AUU* mutants. The localization of Smc4 at the nucleolus does not appear to be affected in these mutants. Arrows denote the nucleolus. Bar, 1 µm.

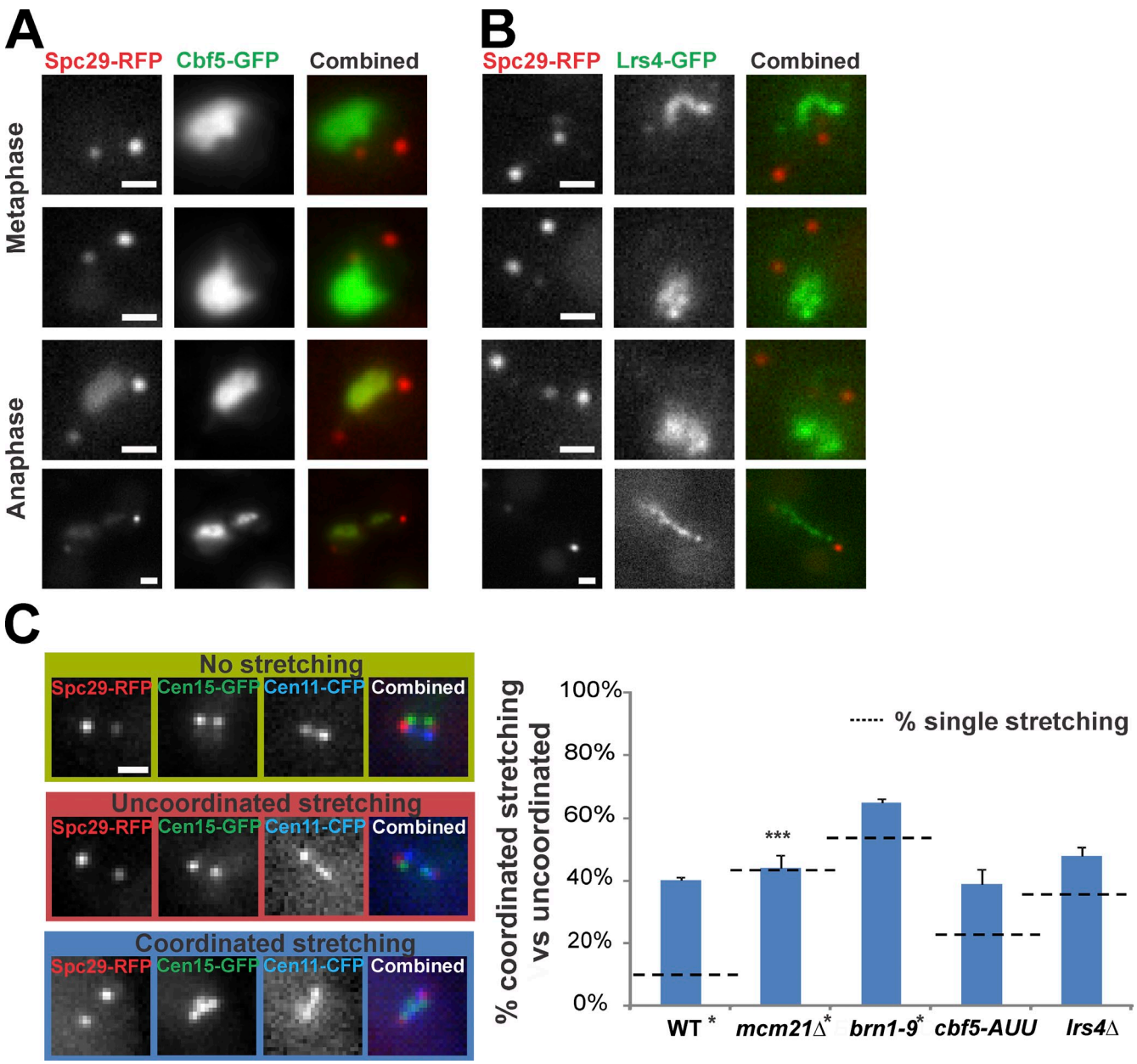

Figure S2. **Localization and function of Cbf5 and monopolin.** (A and B) Cbf5 and monopolin localize primarily to the nucleolus in metaphase. Images of C-terminal GFP-tagged Cbf5 (A) and monopolin subunit Lrs4 (B) in metaphase and anaphase are shown. Both Cbf5 and Lrs4-GFP appear more concentrated in the nucleolus. (C) Coordinated stretching is dependent on pericentric cohesin**.** Cells containing two operator DNA arrays in the pericentromere, TetO arrays 4.5 kb from *CEN11* and LacO arrays 6.8 kb from *CEN15*, were imaged with TetR-CFP and LacI-GFP-NLS, respectively. Pericentromeres were classified as no stretch (both arrays appear as foci), uncoordinated stretching (stretching in only one of the labeled arrays), or coordinated stretching (stretching in both labeled arrays) for WT (n = 267), *mcm21Δ* (n = 352), *brn1-9* (n = 298), *cbf5-AUU* (n = 142), and *lrs4Δ* (n = 179). Coordinated stretching (as determined by the percentage of cells with at least one stretching event that have both arrays stretched; WT, n = 37; *mcm21Δ*, n = 216; *brn1-9*, n = 204; *cbf5-AUU*, n = 43; and *lrs4Δ*, n = 67) is compared with single stretching levels (black dashed lines, indicative of expected coordinated stretching levels if chromosomes behave independently). The triple asterisk denotes statistical similarity between single stretching and coordinated stretching ($\chi^2 > 0.4$). Error bars represent standard deviations. Single asterisks indicate that WT, *mcm21Δ*, and *brn1-9* data in this figure were obtained from Stephens et al. (2013c). Bars, 1 µm.

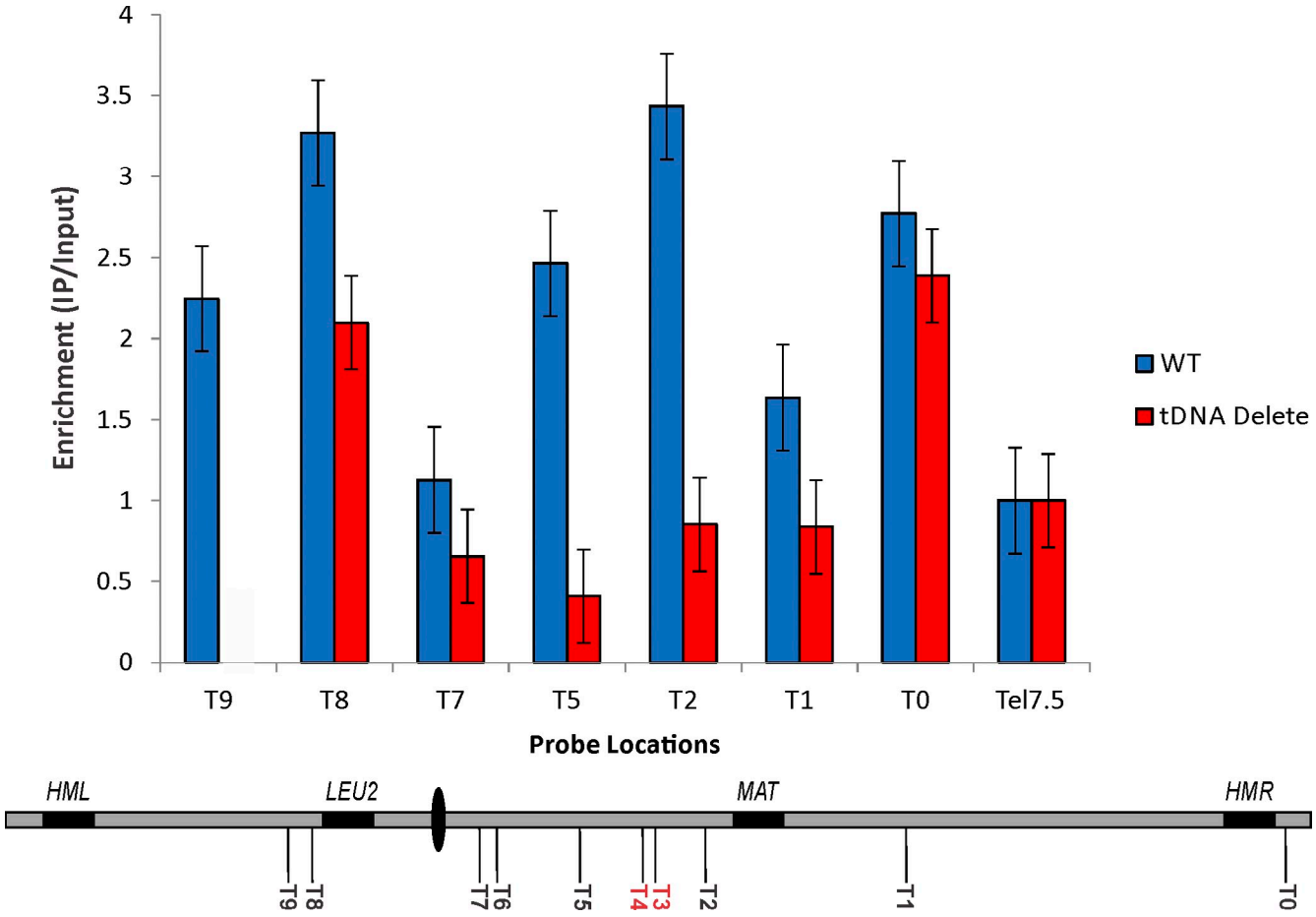

Figure S3. **Quantitative chromatin IP mapping the localization of CBF5-GFP in WT W-303 strains and an isogenic strain lacking the tRNA gene on chromosome III.** Data are shown as the mean enrichment of IP/input normalized to a probe located 7.5 kb from chromosome 6R. Four IPs from two independent cross-links were performed for each strain. Error bars represent standard deviations from the mean. tDNA3 and tDNA4 are absent in W-303. We were unable to map CBF5 at T9 in the tRNA gene-deleted strain because the deletion abolishes the binding site for one of the quantitative PCR primers and for T6 because of LTRs in its vicinity.

Table S1. **Strains used in this paper**

Strain number	Genotype
KBY 9035	(YEF473A) Smc4-GFP-Kan, Spc29-RFP-Hb
KBY 9465	(YHY64a1 MATa ura3-52 lys2-801amber ade2-101ochre trp1-Δ1 his3-Δ200 leu2-Δ1 *cbf5-1*) Spc29-RFP:Hb; *cbf5-1* is a temperature-sensitive mutation in the CBF5 gene (Jiang et al., 1993)
KBY 9405	473A Spc29-RFP:Hb, *lrs4Δ*-Nat, Smc4-GFP-Kan
KBY 9514	(KBY 9035 473A Smc4-GFP-Kan Spc29-RFP:Hb) *cbf5-AUU*–Nat;*Cbf5-AUU* is a mutation in the AUG start codon to AUU (Kendall et al., 2000)
Y3339-1	SH518 background, tsv115(tfc3), pFL44L (empty, URA3); Tfc3-tsv115 is a G349E mutation in the TFC3 gene (Lefebvre et al., 1994)
KBY 9475	(Y3339 SH518 background, tsv115[tfc3], pFL44L [empty, URA3]) Smc4-GFP-Kan Spc29-RFP:Hb
KBY 9472	(YEF 473A) Spc29-RFP:Hb Cbf5-GFP-Kan
KBY 7999	(YEF 473A) Spc29-RFP:Hb
KBY 9075-1	(YEF 473A) Spc29-RFP:Hb Nuf2-GFP-Ura
KBY 9403	(YEF 473A) Spc29-RFP:Hb, *lrs4Δ*-Nat, Nuf2-GFP-Ura
KBY 9476	YHY64a1 MATa ura3-52 lys2-801amber ade2-101ochre trp1-Δ1 his3-Δ200 leu2-Δ1 *cbf5-1* Spc29-RFP-Hb Nuf2-GFP-Ura
KBY 9053-1	(YEF 473A) brn1-9-NAT Spc29-RFP-Hb Nuf2-GFP-Ura
KBY 9496	(YEF 473A) Spc29-RFP:Hb Cse4-2×GFP-Trp (pRB920)
KBY 9492	(YEF 473A) Spc29-RFP:Hb *lrs4Δ*-Nat Cse4-2×GFP-Trp (pRB920)
KBY 9487	YHY64a1 MATa ura3-52 lys2-801amber ade2-101ochre trp1-Δ1 his3-Δ200 leu2-Δ1 *cbf5-1* Spc29-RFP-Hb Cse4-2×GFP-Trp (pRB920)
KBY 9157-1	(YEF 473A) brn1-9-NAT Spc29-RFP-Hb Cse4-2×GFP-Trp
KBY 9121	MATa ade1 met14 ura3-52 leu2-3,112 lys2Δ::lacI-GFP-NLS-NATr his3-11,15 12.5 kb XI::lacO-KANMX NatΔ::His3MX6 Spc29-RFP-Hb
KBY 9132	MATa ade1 met14 ura3-52 leu2-3,112 lys2Δ::lacI-GFP-NLS-NATr his3-11,15 12.5 kb XI::lacO-KANMX NatΔ::His3MX6, Spc29-RFP-Hb *brn1-9*-Nat
KBY 9133	MATa ade1 met14 ura3-52 leu2-3,112 lys2Δ::lacI-GFP-NLS-NATr his3-11,15 12.5 kb XI::lacO-KANMX NatΔ:His3MX6 Spc29-RFP-Hb *mcm21Δ*-Nat
KBY 9533-1	Mata ade1 met14 ura3-52 leu2-3,112 lys2Δ::lacI-GFP-NLS-NATr his3-11,15 12.5 kb XI::lacO-KANMX NatΔ::His3MX6, Spc29-RFP-Hb *cbf5-AUU*-Nat
KBY 9199	CEN15(1.8)-GFP MATa ade2-101 his3-11 trp1-1 ura3-1 leu2-3,112 can1 LacINLSGFP:HIS3 lacO::URA3 (at 1.8 kb from CEN15, 10-kb array) tetO-LEU2 at CEN11 met 14 tetRCFP-Hb, Hb::Kan Spc29RFP:Hb
KBY 9406	CEN15(1.8)-GFP MATa ade2-101 his3-11 trp1-1 ura3-1 leu2-3,112 can1 LacINLSGFP:HIS3 lacO::URA3 (at 1.8 kb from CEN15, 10-kb array) tetO-LEU2 at CEN11 met14 tetRCFP-Hb, Hb::Kan, Spc29RFP:Hb *mcm* Δ-Nat
KBY 9407	CEN15(1.8)-GFP MATa ade2-101 his3-11 trp1-1 ura3-1 leu2-3,112 can1 LacINLSGFP:HIS3 lacO::URA3 (at 1.8 kb from CEN15, 10-kb array) tetO-LEU2 at CEN11 met14 tetRCFP-Hb, Hb::Kan Spc29RFP:Hb, *brn1-9*-Nat
KBY 9408	CEN15(1.8)-GFP MATa ade2-101 his3-11 trp1-1 ura3-1 leu2-3,112 can1 LacINLSGFP:HIS3 lacO::URA3 (at 1.8 kb from CEN15, 10-kb array) tetO-LEU2 at CEN11 met14 tetRCFP-Hb, Hb::Kan Spc29RFP:Hb, *lrs4Δ*-Nat
KBY 9518	CEN15(1.8)-GFP MATa ade2-101 his3-11 trp1-1 ura3-1 leu2-3,112 can1 LacINLSGFP:HIS3 lacO::URA3 (at 1.8 kb from CEN15, 10-kb array) 9tetO-leu at CEN11 met14 tetRCFP-Hb, Hb::Kan Spc29RFP:Hb, *cbf5-AUU*-Nat
KBY 9468-1	(YEF 473A) Spc29RFP:Hb Tfc1-GFP-Kan
KBY 9513	YHY64a1 MATa ura3-52 lys2-801amber ade2-101ochre trp1-Δ1 his3-Δ200 leu2-Δ1 *cbf5-1* Spc29-RFP-Hb Tfc1-GFP-Kan
KBY 9527	(GRY812 MATa tDNA[0–9]D T1/T7::HIS3 ade2-1::LacI-GFP::ADE2 LEU2) Spc29-RFP:Hb, 1.1-kb CEN3::LacO-KAN (1.2-kb array)
KBY 9528	(ROY4810 MATa tDNA[WT] ade2-1::LacI-GFP::ADE2 LYS2) Spc29-RFP:Hb 1.1kbCEN3::lacO-KAN (1.2-kb array)
KBY 9495	(YEF 473A) Spc29-RFP:Hb Tub1-GFP on CEN TRP1 plasmid (pMG2)
KBY 9494	YHY64a1 MATa ura3-52 lys2-801amber ade2-101ochre trp1-Δ1 his3-Δ200 leu2-Δ1 *cbf5-1* Spc29-RFP-Hb Tub1-GFP on CEN TRP1 plasmid (pMG2)
KBY 9187	(YEF 473A) Spc29-RFP-HB Lrs4-GFP-Kan
KBY 9484	(YEF 473A) Smc4-GFP-Kan, Spc29-RFP-Hb, Cbf5-microtubule binding domain truncation-Nat
KBY 9568	(YEF 473A) Smc4-GFP-Kan, Spc29-RFP-Hb, Cdc14-CFP-His
KBY 9571	(KBY 9475 Y3339 SH518 background, tsv115[tfc3], pFL44L [empty, URA3] Smc4-GFP-Kan Spc29-RFP-Hb) Cdc14-CFP-His
KBY 9572	(KBY 9568 Smc4-GFP-Kan Spc29-RFP-Hb Cdc14-CFP-His) *cbf5-AUU*-Nat

References

Jiang, W., K. Middleton, H.J. Yoon, C. Fouquet, and J. Carbon. 1993. An essential yeast protein, CBF5p, binds in vitro to centromeres and microtubules. *Mol. Cell. Biol.* 13:4884–4893.

Kendall, A., M.W. Hull, E. Bertrand, P.D. Good, R.H. Singer, and D.R. Engelke. 2000. A CBF5 mutation that disrupts nucleolar localization of early tRNA biosynthesis in yeast also suppresses tRNA gene-mediated transcriptional silencing. *Proc. Natl. Acad. Sci. USA*. 97:13108–13113. http://dx.doi.org/10.1073/pnas.240454997

Lefebvre, O., J. Rüth, and A. Sentenac. 1994. A mutation in the largest subunit of yeast TFIIIC affects tRNA and 5 S RNA synthesis. Identification of two classes of suppressors. *J. Biol. Chem.* 269:23374–23381.

Stephens, A.D., C.E. Snider, J. Haase, R.A. Haggerty, P.A. Vasquez, M.G. Forest, and K. Bloom. 2013c. Individual pericentromeres display coordinated motion and stretching in the yeast spindle. *J. Cell Biol.* 203:407–416. http://dx.doi.org/10.1083/jcb.201307104